NANO LETTERS

LETTER

pubs.acs.org/NanoLett

Significant Reduction of Thermal Conductivity in Si/Ge Core−Shell Nanowires

Ming Hu,*[,†,§] Konstantinos P. Giapis,[‡,∥] Javier V. Goicochea,[§] Xiaoliang Zhang,[†] and Dimos Poulikakos[†,⊥]

[†]Laboratory of Thermodynamics in Emerging Technologies, Department of Mechanical and Process Engineering, ETH Zurich, 8092 Zurich, Switzerland

[‡]Division of Chemistry and Chemical Engineering, California Institute of Technology, Pasadena, California 91125, United States

[§]IBM Research GmbH, Zurich Research Laboratory, 8803 Rüschlikon, Switzerland

ABSTRACT: We report on the effect of germanium (Ge) coatings on the thermal transport properties of silicon (Si) nanowires using nonequilibrium molecular dynamics simulations. Our results show that a simple deposition of a Ge shell of only 1 to 2 unit cells in thickness on a single crystalline Si nanowire can lead to a dramatic 75% decrease in thermal conductivity at room temperature compared to an uncoated Si nanowire. By analyzing the vibrational density states of phonons and the participation ratio of each specific mode, we demonstrate that the reduction in the thermal conductivity of Si/Ge core−shell nanowire stems from the depression and localization of long-wavelength phonon modes at the Si/Ge interface and of high frequency nonpropagating diffusive modes.

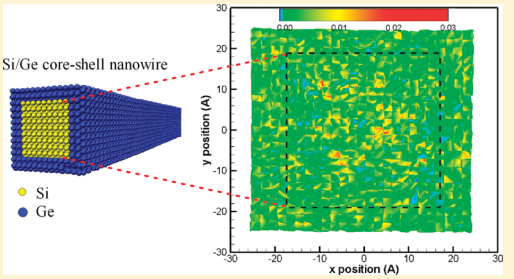

KEYWORDS: Si/Ge core−shell nanowires, thermal conductivity, phonon, heat transfer, thermoelectric materials

The thermoelectric effect manifests itself as the direct conversion of temperature differences to electric voltage in appropriate materials and vice versa. A thermoelectric device can thus in principle improve the thermodynamic efficiency of heat engines by utilizing part of the waste heat to generate electricity. A figure of merit for the energy conversion performance of a thermoelectric material is the dimensionless coefficient, $ZT = S^2\sigma T/\kappa$, where S, σ, T, κ are the Seebeck coefficient, electrical conductivity, absolute temperature, and thermal conductivity, respectively. Greater values of ZT indicate greater efficiency and values in the 3 − 4 range are needed for thermoelectrics to become competitive with other electricity producing methods. The potential of such materials for use is of course higher if the required temperature difference above environmental temperature is not very high. Research to date has focused on reducing the thermal conductivity of thermoelectric materials relative to the bulk by nanostructuring the material (nanowires, superlattices, composite matrices). If the electrical properties are not negatively affected, improved thermoelectric performance should ensue based on the definition of the ZT coefficient. Nanoscale structures with at least one dimension of the order of the phonon mean free path may increase phonon scattering thereby reducing thermal conductivity.

Recent experiments on Si nanowires (NWs) have shown them to be promising thermoelectric structures, specifically because of the reduction in thermal conductivity from increased phonon scattering at the confining walls.[1] Additional methods to reduce the thermal conductivity have been proposed, supported by simulations. Donadio et al.[2] found that Si NWs with amorphous surface have thermal conductivity of about 100 times lower than bulk silicon. They suggested that heating the Si NW up to a temperature very close to its melting point followed by quenching at an extremely fast cooling rate may help render the nanowire surface amorphous. Chen et al.[3] proposed recently to increase phonon scattering by considering a small hole at the center of thin (cross section of 2.72 × 2.72 nm) Si NWs to form a nanotube. Their simulations suggest that a 1% reduction in the NW cross section can cause a 35% reduction in room-temperature thermal conductivity. While this result is promising, drilling consistently a small hole in the center of such a Si NW poses a substantial barrier to realizing the proposed concept structure. Surface roughness has been shown in experiments[1] to reduce significantly the thermal conductivity in Si nanowires, but the mechanism of phonon transport suppression has yet to be elucidated.[4]

We present herein results from molecular dynamics (MD) simulations of phonon propagation in Si/Ge core−shell nanowires. Our calculations show that a Ge shell of only 1 to 2 unit cell (uc) thickness can lead to a dramatic 75% decrease in thermal conductivity at room temperature as compared to an uncoated single-crystalline Si NW. By analyzing the vibrational density states of phonons and the participation ratio of each specific mode, we demonstrate that the reduction in the thermal conductivity of Si/Ge core−shell nanowire stems from the depression and localization of long-wavelength phonon modes at the Si/Ge interface and also of high frequency nonpropagating diffusive modes. The proposed core−shell nanowire may be

Received: October 22, 2010
Revised: November 30, 2010
Published: December 9, 2010

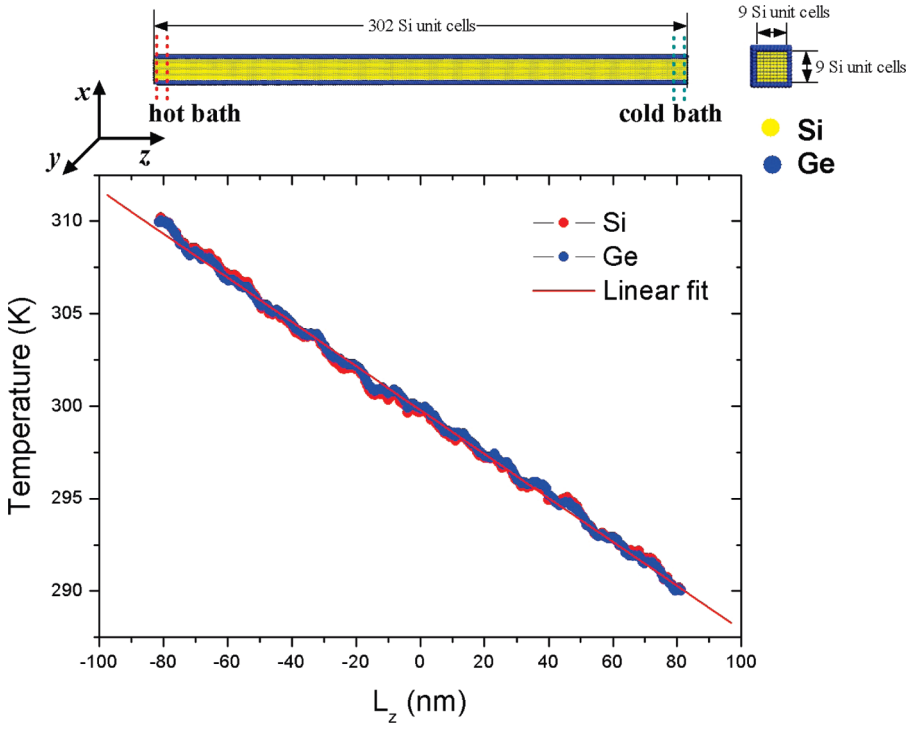

Figure 1. (Top) Side and cross-sectional view of the Si/Ge core−shell nanowire with 9 × 9 × 302 unit cells of Si core covered by 1 unit cell of Ge. Color coding: yellow, Si; blue, Ge. (Bottom) The corresponding temperature profiles for the Si core and Ge shell. The solid line is a linear fit to the average of the two temperature profiles.

realized experimentally as evidenced by existing nanowire structures of this kind reported in the literature.[5,6]

Our model system consists of a single-crystalline Si NW covered by a Ge layer. The longitudinal direction is set along the z axis, so that atoms in the same layer have the same z coordinate. The initial Si nanowire (160 nm long) is constructed from diamond-structured bulk silicon with $n \times n \times 302$ unit cells in the x, y, and z directions, where n = 6, 9, 12, and 20, corresponding to a cross-sectional width of 2.3, 3.5, 4.6, and 7.7 nm, respectively. After constructing the Si NW, the Ge layer was built on each Si NW surface with the same orientation as the Si NW. The number of Ge unit cells in x and y directions was varied from 1 to 4, while the number in the z direction was 290, taking into consideration the [001] lattice mismatch between Si and Ge. The Ge atoms were allowed to reach their equilibrium positions, determined by the model potentials chosen (see below). Strained epitaxial Ge layers were also considered but the results did not change substantially. A schematic of the nanowire structure is shown in the top panel of Figure 1. In all cases, both the Si NW and the Ge layer axes lie along the [001] crystal axis of the diamond lattice. The surfaces in transverse directions (x and y axes) for both Si and Ge are each (110) type. This particular choice was made because nanowires with (100)-type surfaces, which are quite high energy when not reconstructed, were found to become amorphous under MD annealing. The (110) surface, on the other hand, has 3-fold-coordinated surface atoms and is lower in energy than the unreconstructed (100) surface. It is thus more likely to form in experiments. Nanowires made with this surface termination were found to be stable with respect to disordering or surface reconstructions up to MD simulation temperatures of 500 K and perhaps beyond.[7]

In all MD simulations performed herein, the Stillinger-Weber (SW) potential was used to calculate the thermal conductivity of the Si/Ge NWs with the diamond structure. This potential uses two-body and three-body terms to stabilize the diamond lattice. The original parameters were developed to provide an approximate description of condensed phases of Si.[8] Parameters for Ge were determined by fitting to experimental data.[9] In the simulation studies described here, the parameters of refs 8 and 9 were adopted to describe Si−Si and Ge−Ge interactions. Parameters for Si−Ge interactions were obtained by taking the arithmetic mean of Si and Ge parameters for σ_{Si-Ge} and the geometric mean for λ_{Si-Ge} and ε_{Si-Ge}, as suggested in the literature.[10,11] This model has been used to predict the thermodynamic properties of Si,[12,13] Ge,[14] and bulk Si−Ge alloys[15] and also the thermal transport properties of Si/Ge superlattices,[16] composites,[17] and nanowires.[18]

All MD calculations were performed using the LAMMPS[19] package with a time step of 1 fs throughout. In the first stage of MD simulations, the system was equilibrated with free boundary conditions in all directions, corresponding to zero pressure, and a constant temperature of T = 300 K for 5 ns using Nosé−Hoover temperature thermostat.[20] After the constant temperature relaxation, we continued to relax the system with *NVE* (constant volume and no thermostat) ensemble for 1 ns. This was done by freezing one unit cell of boundary atoms at the two ends of the Si nanowire. During this stage, the total energy and temperature of the system were monitored. We found that the total energy was conserved and the temperature of the entire system remained constant with fluctuations around 300 K, which meant that the system had reached the equilibrium state.

Following equilibration, we computed the thermal conductivity of the system with nonequilibrium MD. To establish a temperature gradient along the longitudinal direction, the atoms

dx.doi.org/10.1021/nl103718a |*Nano Lett.* 2011, 11, 618–623

close to the two ends of the NW (about 8 unit cells long) were placed into hot and cold baths with temperatures T_L and T_R for the left and right end, respectively, as shown in the top panel of Figure 1. Nosé−Hoover heat baths were applied. It has been previously shown that the thermal conductivity results are independent of the heat bath used (Nosé−Hoover or Langevin).[18] The total heat flux in the longitudinal direction is defined as[21]

$$J_L(t) = \frac{1}{V}\left[\sum_i v_{i,L}\varepsilon_i + \frac{1}{2}\sum_{i,j,i\neq j} r_{ij,L}(\vec{f}_{ij}\cdot\vec{v}_j) + \sum_{i,j,k} r_{ij,L}(\vec{f}_j(ijk)\cdot\vec{v}_j)\right] \quad (1)$$

where the subscript "L" denotes a quantity in the longitudinal direction, v_i is the velocity of atom i, ε_i is local site energy, r_{ij} is the relative distance between atom i and j, $\vec{f}_{ij}$ is the two-body force between atom i and j, $\vec{f}_j$ (ijk) is the three-body interactions between atoms i, j, and k, and V is the volume of the region selected to calculate the heat flux. Note that we exclude the regions ($\sim$ 10 unit cells long) close to both ends and compute the heat current only for the rest of the NW to avoid the nonlinear effect of the heat source and heat sink at the ends. Simulations were carried out long enough (about 15 ns) for the system to reach steady state conditions, where a constant local heat flux is established in the longitudinal direction. After that, a time averaging of temperature and heat flux was performed for an additional 15 ns. Figure 1 illustrates a typical time-averaged temperature profile used to compute the thermal conductivity. Thermal boundary resistance effects are avoided by fitting the middle region of the temperature profile with a linear function. The resulting temperature gradient is used to calculate the thermal conductivity as

$$\kappa = -\frac{\overline{J}_L}{\partial T/\partial z} \quad (2)$$

where $\overline{J}_L$ is the averaged heat flux in the longitudinal direction and $\partial T/\partial z$ is the temperature gradient determined from the linear fitting. Our simulation result of 9.1 $\pm$ 0.84 W/mK for 6 $\times$ 6 unit cell cross section and 160 nm long Si NW is consistent with Yang's MD result,[22] who reported a thermal conductivity of $\sim$6 $\pm$ 1 W/mK for the same cross section and 150 nm long Si NW. Considering that the [110] surface we used results in less scattering than the [100] surface they used, it is reasonable to expect a slightly higher thermal conductivity. In addition, our simulation result of 20.2 $\pm$ 0.78 W/mK for 4.6 nm thick 160 nm long Si NW is in good agreement with Ponomareva's work[23] where 20 W/mK was predicted by MD simulation for 4.2 nm thick 125 nm long Si NW. The theoretical calculations in ref 24, as clearly stated by the authors of this reference, are expected to be valid for considerably wider nanowires (above 35 nm, for which confinement effects are unimportant) than those studied in our work. It is worth noting in this respect that the values of the boundary scattering parameter in the model of ref 24 were assigned so as to represent the very diffusive nature of the rough and likely oxidized boundary in the experiments of ref 25. In our MD study as well as in the other MD studies mentioned above, which are in agreement with ours, this is not the case as we necessarily simulate a perfect Si atomic structure with atomically smooth surface. We also noticed that our MD results are higher than experimental values for individual Si NWs.[25] The discrepancy can be attributed to defects, impurities, surface roughness, and oxidation present in the experimental samples, which may impact adversely the nanowire's thermal conductivity. In contrast, theoretical calculations assume that the Si NWs are perfect crystals with atomically smooth surfaces, which facilitate heat conduction.

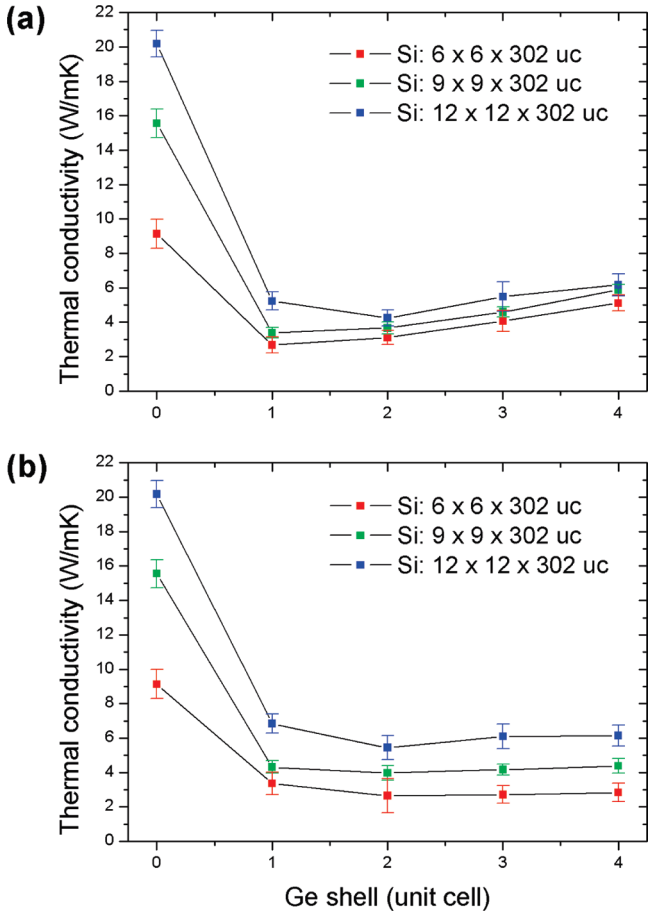

Figure 2. (a) Overall thermal conductivity of the Si/Ge core−shell nanowire as a function of the number of layers in the Ge shell for different cross-sectional areas of the Si core. (b) Thermal conductivity of only the Si core in the Si/Ge core−shell structure, plotted as in (a).

The dependence of the thermal conductivity on the number of Ge shell layers is shown in Figure 2. Remarkably, the addition of the Ge shells lowers substantially the thermal conductivity of the core−shell structure thus formed, as compared to that of the pure crystalline Si nanowire. Even calculating the thermal conductivity of only the Si core, the drop is significant for all cross sections studied. The largest drop in the thermal conductivity of 75% occurs for the Si core with the 9 $\times$ 9 cross-section, when covered by only two atomic layers of Ge. For the Si nanowires with 6 $\times$ 6 and 12$\times$12 cross-section, the thermal conductivity is reduced by about 70%. These values are a factor of 2 lower than the thermal conductivities achieved by assuming the existence of a longitudinal hole at the nanowire center,[3] a structure believed to be markedly more difficult to fabricate than the Si/Ge core−shell nanowire[5,6] investigated herein. Growing a Ge layer onto the Si NW surface does not change the Si core much and it will not have a negative impact on its electrical conductivity.

We note that the overall thermal conductivity of the entire core−shell NW increases slightly as more Ge layers are added. This effect originates in the progressively larger contribution of thicker Ge layers to the overall heat transfer. The minimum of the overall thermal conductivity occurs at a Ge thickness of one unit cell for the 6 $\times$ 6 and 9 $\times$ 9 Si NWs, and at two unit cells for the 12 $\times$ 12 Si NW. Moreover, the overall thermal conductivity curves for all

dx.doi.org/10.1021/nl103718a |*Nano Lett.* 2011, 11, 618–623

Table 1. Reduction in Overall Thermal Conductivity for the Si/Ge Core−Shell Composite versus That Only for the Si Core, As Compared to the Thermal Conductivity for an Uncoated Si Core for Nanowires of Various Thickness and Length[a]

size of Si core	reduction percentage in overall thermal conductivity of the Si/Ge composite	reduction percentage in thermal conductivity of the Si core
9 × 9 × 302 uc	76.5%	75.0%
16 × 16 × 302 uc	73.9%	64.5%
20 × 20 × 302 uc	70.1%	59.3%
9 × 9 × 402 uc	73.7%	71.0%
9 × 9 × 502 uc	71.4%	69.3%
9 × 9 × 602 uc	71.1%	69.1%

[a] For all cases, a Ge shell of 2 unit-cells (uc) thickness was used. For the Si core, 20 uc corresponds to a thickness of 7.7 nm and 602 uc corresponds to a length of 327 nm.

core−shell cases are close in magnitude and vary similarly with shell thickness, possibly because the presence of the Ge shell interferes with heat transfer in both the Si core and the Ge shell. In contrast, the thermal conductivity of the Si core taken alone (see Figure 2b) exhibits a weaker dependence on shell thickness, while its magnitude is more spread out for the different cross sections. Since thicker Ge shells do not reduce further the Si NW conductivity, there must exist a maximum interference depth for each Si core. From the minimum thermal conductivity of the Si core in Figure 2b, we estimate the maximum depth to be about 2−4 unit cells of Si for the three different Si NW sizes considered. For example, a Ge shell of two unit-cell thickness can reduce the thermal conductivity of a 9 × 9 and 12 × 12 Si NW to that of a 2 × 2 and 4 × 4 Si NW, respectively. Previous studies[22,26] have shown that the thermal conductivity of Si NWs depends not only on the NW length, but also on the cross-sectional area (approximately proportional). Thus, the thermal conductivity of a 2 × 2 Si NW should be 22% of that for 9 × 9, which again is consistent with the MD results. This behavior may appear counterintuitive: two noninterfering parallel NWs should always yield an increase in the overall thermal conductivity, as is observed for the electrical conductivity. Assuming no interference, the overall thermal conductivity of a 9 × 9 Si NW covered by 2-unit-cells Ge[27] should be about $\kappa_{overall} = 0.48\kappa_{Si} + 0.52\kappa_{Ge} = 13.9$ W/mK. This value should be contrasted with the MD calculated thermal conductivity of 3.7 W/mK when interference at the interface is taken into consideration. We also calculated the overall thermal conductivity using the generic phonon transport model proposed in ref 28 and obtained a value of 14.0 W/mK, which is still quite different from our MD simulation result.

The effect of the cross-sectional area and length has also been considered. The results are compared in Table 1. The reduction in thermal conductivity of both the Si/Ge core−shell NW and the Si core alone is less for larger cross sections and longer lengths, but the effect remains significant. This can be explained by considering that the surface-to-volume ratio decreases with wire thickness, thus, the interfacial area affected by the Ge coating is relatively smaller in thicker wires, leading to higher thermal conductivity for the Si core. We note, however, that for the largest cross section case (possible for our computational resources) corresponding to a thickness of 7.7 nm, the thermal conductivity of the Si core can still be reduced by about 60%. By extrapolating the calculated data points, we speculate that the thickness where

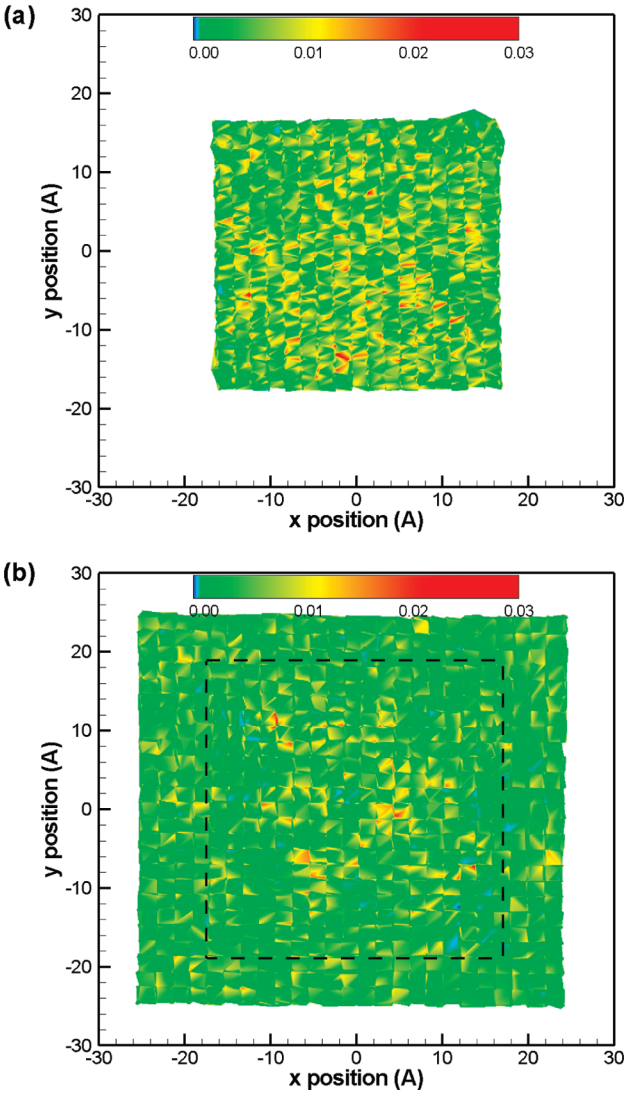

Figure 3. Contour of local heat flux across a plane at $z = 0$ for (a) the pure Si nanowire, and (b) the composite Si/Ge nanowire covered by two layers of Ge. The core Si is a matrix of 9 × 9 × 302 Si unit cells. The dashed line represents the Si/Ge interface to guide the eye. The high positive value defines the high heat flux in the longitudinal (z) direction.

the reduction percentage becomes insignificant should be around 24 nm. The length dependence of the thermal conductivity has been reported in the literature.[29] The slope of the thermal conductivity with respect to length starts to diverge in the range of 217 to 272 nm for the 9 × 9 cross section, which is consistent with a previous study.[22]

To reveal how the Ge shell affects heat transfer in the Si NW, we define the "local" heat flux on a single atom by determining the contribution of every atom to each term in eq 1.[21] Taking the case of the 9 × 9 Si NW with a layer of 2-unit-cells of Ge, we calculated the average local heat flux in the longitudinal (z) direction for a selected segment, ranging from −50 to +50 Å. The volume of the selected segment is used to calculate the local heat flux. We then projected the local heat flux magnitude of the selected atoms to the XY plane at $z = 0$ to generate an intensity contour as shown in Figure 3. In the uncoated Si NW, regions of high and low heat flux are distributed uniformly over the entire cross-sectional area, with the exception of surface regions where the vibrational modes of atoms are more

dx.doi.org/10.1021/nl103718a |*Nano Lett.* 2011, 11, 618–623

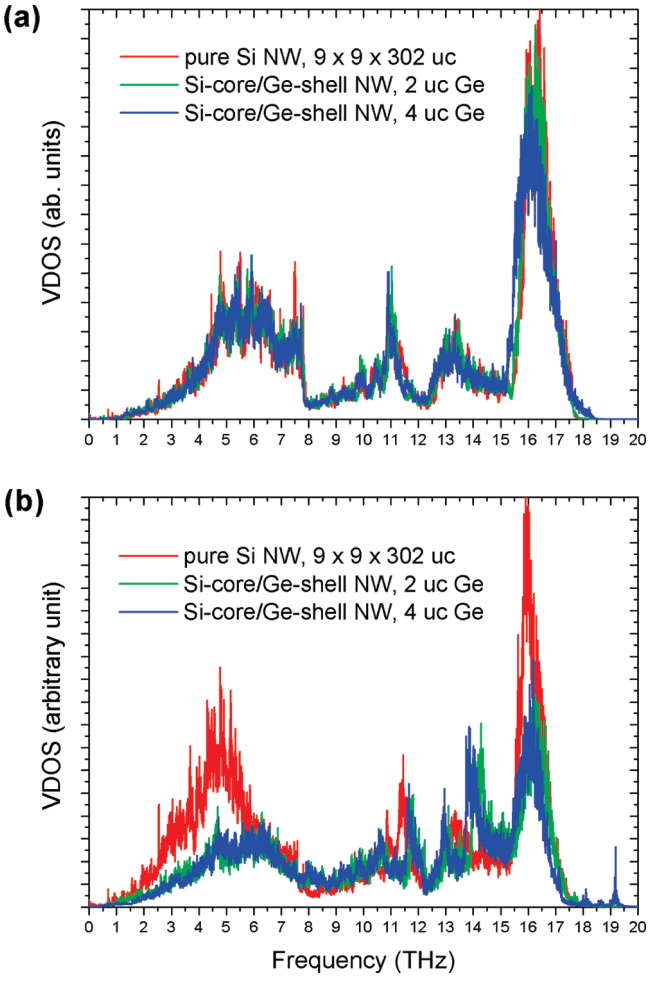

Figure 4. Comparison of vibrational density of states in Si nanowires in the absence and presence of a Ge shell of 2 and 4 unit cell thickness. (a) VDOS of Si atoms located in the center of the Si core; (b) VDOS of Si atoms located at the Si/Ge interface.

localized. In contrast, the heat flux profile in the Si/Ge core−shell NW shows a different feature: heat transfer appears to occur over most of the cross-sectional area at low flux, while *only* the central region is capable of dissipating heat at high flux. A comparison of Figure 3, panels a and b, clearly shows that the presence of the Ge shell influences adversely the thermal transport properties of the Si core.

The reduction in thermal conductivity of the Si NW can be correlated with the depression in the vibrational density of states (VDOS) of Si atoms on the nanowire surface upon addition of the Ge shell. The VDOS is calculated by a Fourier transform of the atomic velocity autocorrelation function and the results for selected Ge shells are shown in Figure 4. For Si atoms in the center of the Si core (Figure 4a), the VDOS does not change much with added Ge layers, as expected from bulklike behavior away from the surface. In contrast, the VDOS for Si atoms proximal to the Si/Ge interface exhibits a significant depression of the low frequency part, especially below 6 THz, originating in the lattice mismatch and different atom mass between the Si core and the Ge shell. Given that these low frequency modes are more delocalized, the large extent to the depression of long-wavelength phonon modes must impact adversely the thermal conductivity. Interestingly, the high frequency part of the VDOS in Figure 4b is

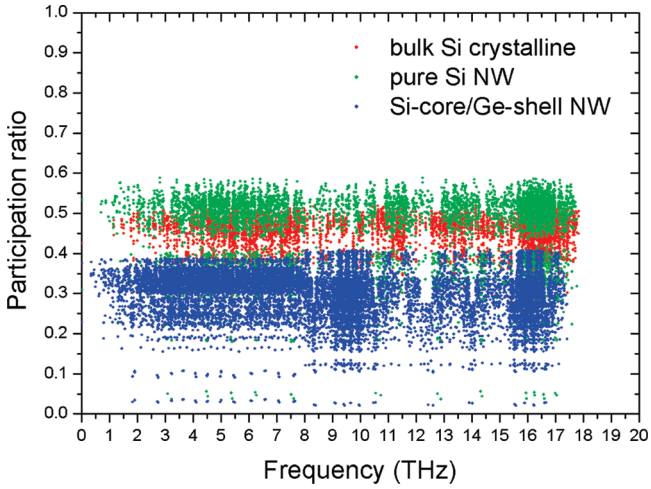

Figure 5. Participation ratio of each vibrational eigen-mode for bulk Si, a pure Si nanowire, and a Si/Ge core−shell composite.

also reduced, especially between 16−17 THz, even for very thin Ge shells. The depression of the high frequency phonons also contributes to the reduction in thermal conductivity, since these nonpropagating, diffusive modes can also carry heat in the core−shell NW, as it has been shown earlier.[2]

The VDOS and the local VDOS provide information averaged over all vibrational modes present in the structure. In contrast, the participation ratio p_λ, characterizes each mode individually and serves as a useful discriminant of spatial localization. p_λ is defined for each eigen-mode λ as[30]

$$p_\lambda^{-1} = N \sum_i \left(\sum_\alpha \varepsilon^*_{i\alpha,\lambda} \varepsilon_{i\alpha,\lambda} \right)^2 \qquad (3)$$

where i sums over all the atoms studied, α is Cartesian direction and sums over x, y, z, $\varepsilon_{i\alpha,\lambda}$ is the vibrational eigenvector component corresponding to the λ^{th} normal mode, and N is the total number of atoms. The participation ratio describes the fraction of atoms participating in a particular mode and, hence, it varies between $O(1)$ for delocalized states to $O(1/N)$ for localized states.[30] We selected a segment of 9 × 9 × 6 Si NW covered by 2 unit cells of Ge, which mimics the long core−shell NW by using periodic boundary conditions in the longitudinal direction, and carried out a vibrational eigen-mode analysis for both the pure Si and the composite Si/Ge. Such eigen-mode analysis involves diagonalizing very large matrices and could be done only for systems of limited size. The largest system analyzed contained a total of N = 4056 atoms of Si and Ge.

In Figure 5, we compare the participation ratio of each vibrational eigen-mode for the pure Si vs the composite Si/Ge nanowire. For reference, we also present results for a 9 × 9 × 6 bulk Si. The participation ratio of bulk Si falls in the range of 0.5−0.6, which is consistent with the literature.[30] Comparing the pure Si nanowire to bulk Si, the participation ratio of vibrational eigen-modes for the former splits into two parts for both low and high frequency phonons: one part resides in the same range as bulk Si, which corresponds to the modes of participating internal atoms; the other part is in the range of 0.3−0.4, corresponding to vibrations of participating surface atoms. The latter surface modes are more localized, causing a reduction in the thermal conductivity of the nanowire. For composite Si/Ge nanowires, Figure 5 makes it clear that almost all the participation ratios are significantly

dx.doi.org/10.1021/nl103718a |*Nano Lett.* 2011, 11, 618–623

reduced in comparison to the pure Si NW and bulk Si. This behavior indicates that the majority of the eigen-modes in the core−shell NW are more localized. Since localized modes are less effective than delocalized modes in facilitating heat transport,[3] it follows that a reduction in thermal conductivity must be expected relative to pure Si NW.

In summary, nonequilibrium molecular dynamics simulations suggest that Ge-coated Si nanowires should exhibit a significant reduction in thermal conductivity relative to uncoated ones. Only a couple of Ge layers can lower the thermal conductivity of Si nanowires by up to 75%, while thicker layers do not actually extend this effect. By analyzing the cross-sectional local heat flux distribution, the phonon vibrational density of states, and the participation ratio of each specific mode, we concluded that the mechanism behind the dramatic reduction in thermal conductivity of the core−shell nanowire is the significant depression and localization of long-wavelength phonon modes in the Si/Ge interface, combined with the depression of high frequency nonpropagating diffusive modes. Thus, simple, realizable coatings on Si and other nanowires are predicted to improve markedly the energy conversion efficiency of nanostructured thermoelectrics.

AUTHOR INFORMATION

Corresponding Author

*E-mail: hum@ethz.ch.

Notes

[||]E-mail: giapis@cheme.caltech.edu.

[⊥]E-mail: dimos.poulikakos@ethz.ch.

ACKNOWLEDGMENT

K.P.G. expresses his gratitude to ETH Zürich for a visiting professorship grant. J.V.G. recognizes the support of European Commission under the Nanopack project of the Seventh Framework Programme (2007−2013). Computational support from the Brutus Cluster at ETH Zurich is gratefully acknowledged. This work was supported by a grant from the Swiss National Supercomputing Centre-CSCS under Project ID s243.

REFERENCES

(1) Hochbaum, A. I.; Chen, R.; Delgado, R. D.; Liang, W.; Garnett, E. C.; Najarian, M.; Majumdar, A.; Yang, P. *Nature* **2008**, *451*, 163.
(2) Donadio, D.; Galli, G. *Phys. Rev. Lett.* **2009**, *102*, No. 195901.
(3) Chen, J.; Zhang, G.; Li, B. W. *Nano Lett.* **2010**, *10*, 3978.
(4) Hippalgaonkar, K.; Huang, B. L.; Chen, R. K.; Sawyer, K.; Ercius, P.; Majumdar, A. *Nano Lett.* **2010**, *10*, 4341.
(5) Lu, W.; Xiang, J.; Timko, B. P.; Wu, Y.; Lieber, C. M. *Proc. Natl. Acad. Sci. U.S.A.* **2005**, *102*, 10046.
(6) Xiang, J.; Lu, W.; Hu, Y.; Wu, Y.; Yan, H.; Lieber, C. M. *Nature* **2006**, *441*, 489.
(7) Becker, B.; Schelling, P. K.; Phillpot, S. R. *J. Appl. Phys.* **2006**, *99*, No. 123715.
(8) Stillinger, F. H.; Weber, T. A. *Phys. Rev. B* **1985**, *31*, 5262.
(9) Ding, K.; Anderson, H. C. *Phys. Rev. B* **1986**, *34*, 6987.
(10) Roland, C.; Gilmer, G. H. *Phys. Rev. B* **1993**, *47*, 16286.
(11) Karimi, M.; Kaplan, T.; Mostoller, M.; Jesson, D. E. *Phys. Rev. B* **1993**, *47*, 9931.
(12) Gomes, C. J.; Madrid, M.; Goicochea, J. V.; Amon, C. H. *J. Heat Transf.* **2006**, *128*, 1114.
(13) Goicochea, J. V.; Madrid, M.; Amon, C. *J. Heat Transf.* **2010**, *132*, No. 012401.
(14) Laradji, M.; Landau, D. P.; Dunweg, B. *Phys. Rev. B* **1995**, *51*, 4894.
(15) Skye, A.; Schelling, P. K. *J. Appl. Phys.* **2008**, *103*, 113524.
(16) Landry, E. S.; McGaughey, A. J. H. *J. Appl. Phys.* **2010**, *107* No. 013521.
(17) Huang, X. P.; Huai, X. L.; Liang, S. Q.; Wang, X. W. *J. Phys. D: Appl. Phys.* **2009**, *42*, No. 095416.
(18) Chen, J.; Zhang, G.; Li, B. W. *Appl. Phys. Lett.* **2009**, *95*, No. 073117.
(19) Plimpton, S. *J. Comput. Phys.* **1995**, *117*, 1.
(20) (a) Nosé, S. *J. Chem. Phys.* **1984**, *81*, 511. (b) Hoover, W. G. *Phys. Rev. A* **1985**, *31*, 1695.
(21) Schelling, P. K.; Phillpot, S. R.; Keblinski, P. *Phys. Rev. B* **2002**, *65*, No. 144306.
(22) Yang, X.; To1, A. C.; Tian, R. *Nanotechnology* **2010**, *21*, No. 155704.
(23) Ponomareva, I.; Srivastava, D.; Menon, M. *Nano Lett.* **2007**, *7*, 1155.
(24) Mingo, N. *Phys. Rev. B* **2003**, *68*, 113308.
(25) Li, D.; Wu, Y.; Kim, P.; Shi, L.; Yang, P.; Majumdar, A. *Appl. Phys. Lett.* **2003**, *83*, 2934.
(26) Wang, S. C.; Liang, X. G.; Xu, X. H.; Ohara, T. *J. Appl. Phys.* **2009**, *105*, No. 014316.
(27) The thermal conductivity of a Ge nanowire is calculated to be about 80% of that for a Si nanowire of the same cross-section.
(28) Yang, R.; Chen, G.; Dresselhaus, M. S. *Nano Lett.* **2005**, *5*, 1111.
(29) Yang, N.; Zhang, G.; Li, B. W. *Nano Today* **2010**, *5*, 85.
(30) Bodapati, A.; Schelling, P. K.; Phillpot, S. R.; Keblinski1, P. *Phys. Rev. B* **2006**, *74*, No. 245207.

NOTE ADDED AFTER ASAP PUBLICATION

The formula just below the table on page 4 was modified in the version of this paper published on December 9, 2010. The correct version published December 27, 2010.